

## STRENGTH EVALUATION OF BERYLLIUM WINDOW FOR SPRING-8 FRONT ENDS

Sunao Takahashi, Tetsuro Mochizuki  
 SPring-8/JASRI - Mikazuki –Hyogo 679-5198 - Japan  
 Hideo Kitamura  
 SPring-8/RIKEN - Mikazuki –Hyogo 679-5148 - Japan

### Abstract

We carried out an elastic and plastic analysis successfully against a new type beryllium window for the SPring-8 front ends. The new window has beryllium foils of high-purity and fine-surface-roughness on user's demand. It was confirmed that the new foil has only about half the mechanical strength of the existing one by a static tensile test. Based on the analysis solutions and the tensile test results, we tried to predict the fatigue life of the new window. According to the Manson's universal slope rule, the life was estimated at about  $10^6$  cycles, which is considered to be too enough for the usage.

### 1. Introduction

The beryllium window assembly for the SPring-8 front ends, which is installed at about 35 m away from the light source point, works to separate the ring vacuum from the optics vacuum at X-ray beamlines. As shown in Figure 1, the assembly has two beryllium foils of 250  $\mu$  each, and the intermediate area between them is evacuated by an ion pump. The beryllium foil, whose diameter is 18 mm, is attached to a water-cooling copper holder concentrically by brazing or diffusion bonding. As the aperture size of the holder is 10mm, the peripheral area of 4 mm on each side is fixed on the copper holder. The maximum beam size onto the beryllium foil, which is shaped by the XY slit assembly, is usually about 1.2 mm square. The temperature of the central area in the foil increases locally by an irradiation of such a sharp beam, resulting in the radical expansion of the foil. On the other hand, as the peripheral region is fixed on the cooling copper body, the compressive stress will occur. Therefore, it is important to conduct a thermo-mechanical analysis and to evaluate the solution on the basis of the practical mechanical properties of the material. To reduce the heat loads on beryllium windows, we prepared the graphite filter assembly, which cut the lower energy part of the X-ray beam. It consists of three axes, each of which has a graphite foil of 100  $\mu$ , and it can be selected either inserted or not inserted condition by stepping motors. Therefore, we can place a maximum thickness of 300  $\mu$  of graphite into the beam by 100  $\mu$  steps.

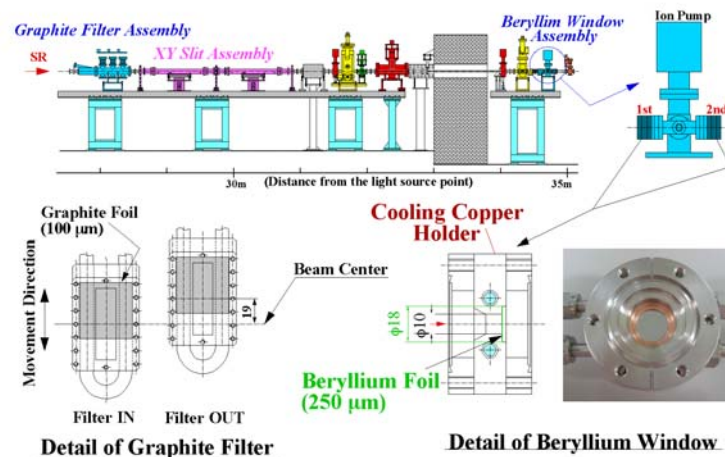


Fig.1: Downstream-side arrangement of the front-end components and details of the beryllium window and the graphite filter.

In the beginning stage, we adopted a popular beryllium foil manufactured as a material of a general X-ray window, which is referred to as TYPE A. Figure 2 shows the relationship between the absorbed power in the TYPE A beryllium foil and the maximum equivalent stress calculated by ANSYS analysis. We have confirmed that if an absorbed power in the TYPE A foil is less than about 12 W, the maximum equivalent stress does not exceed the 0.2% proof stress of about 280 MPa. Accordingly, we regulated the absorbed power in the beryllium foil to be less than 12 W with a combination of graphite filters.

However, some users have requested us to enhance the quality of the beryllium foil. For example, imaging or topography users' request is an improvement of inhomogeneous beam such as unwanted intensity modulations, which causes incoherency. XAFS users demand a betterment of the purity of beryllium to reduce a background near absorption edges. To cope with their demand, we prepared a high-purity and fine-surface-roughness foil. We refer to it as TYPE B. Specifications of both foils are shown in this table.

Table 1: Specifications of the beryllium foils for TYPE A and TYPE B.

	TYPE A	TYPE B
Purity	98.5%	99.8%
Surface Roughness	(Ra >1)	Ra 0.05~0.1
Manufacturing Method	Forging	Casting & Extruding

SPring-8 optics group confirmed one of improvements by comparing refractive contrast imaging of not only both type foils but also the graphite filter [1]. Their desirable arrangement for the front-end filter components consists of only TYPE B beryllium windows without any other filters.

But, new problems were encountered, because the mechanical strength of TYPE B was predicted to be fairly lower than the conventional foil of TYPE A due to the difference of the manufacturing method. To achieve high purity, we adopted the base metal whose manufacturing method consists of casting and extruding instead of the powder forging technology of TYPE A. The manufacturer said that this alteration would bring the reduction of mechanical strength qualitatively. Besides, there was a possibility that the polishing degree would influence on the mechanical properties. However, there was no practical data.

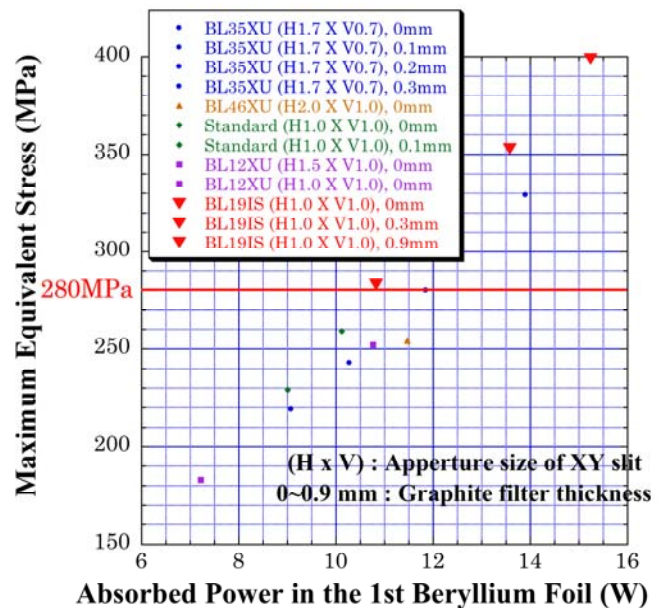


Figure 2: Relationship between the absorbed power and the equivalent stress for TYPE A beryllium window by ANSYS solutions for some cases of several beamlines.

## 2. Static Tensile Tests

We conducted a static tensile test for TYPE B foil to get the practical mechanical properties, such as Young's module, 0.2 % proof stress, tensile strength, and elongation. Figure 3 shows the drawing of a test piece. When preparing the test pieces, the same heat hysteresis as the diffusion bonding in the real process was applied after machining. Since the mechanical properties are temperature-dependent, we measured both at the room temperature and 200°C. Table 2 shows the typical test results and also the data for TYPE A quoted from the manufacturer's brochure. It was confirmed that TYPE B has only about half the mechanical strength of TYPE A.

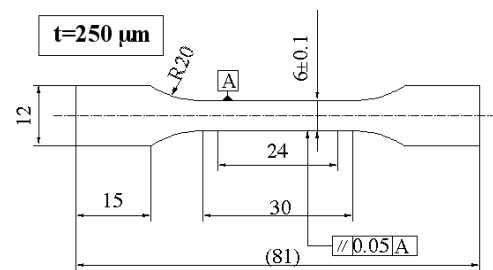


Figure 3: Drawing of a test piece

Table 2: Results of the static tensile test.

	Temperature	Young's Module	0.2% Proof Stress	Tensile Strength	Elongation
TYPE B	22°C	$2.4 \times 10^5$ MPa	183 MPa	335 MPa	8.5%
TYPE B	200°C	$2.1 \times 10^5$ MPa	127 MPa	252 MPa	55.9%
*1 (TYPE A)	RT	$2.7 \sim 3.2 \times 10^5$ MPa	> 280 MPa	> 490 MPa	> 5%

## 3. Analysis

### 3.1. Modelling and Boundary Conditions

We conducted ANSYS analysis on the maximum heat load condition for the SPring-8 standard in-vacuum undulator, which produces a total power of 13.7 kW with a peak power density of more than 500 kW/mrad<sup>2</sup>. On this condition, the peak power density at the beryllium window reaches 450 W/mm<sup>2</sup>, and the partial power onto the first window, after passing through the XY slit aperture size of 1 mm, is about 600 W. As shown in Figure 4, we made a quarter model of the window, and the absorbing region was meshed by dividing into 50 μm each in all directions. The boundary conditions for input power was decided depending on both the energy spectrum at the center of each element and the absorption coefficient of beryllium. The input power was given as the heat generation of each element, which is within the range of about 30 to 40 W/mm<sup>3</sup>. Consequently, the total absorbed power in the whole beryllium window, not the quarter model, is about 12 W. As to the cooling boundary conditions, the temperature of the outside surfaces of the copper holder remains constant at 32.3°C.

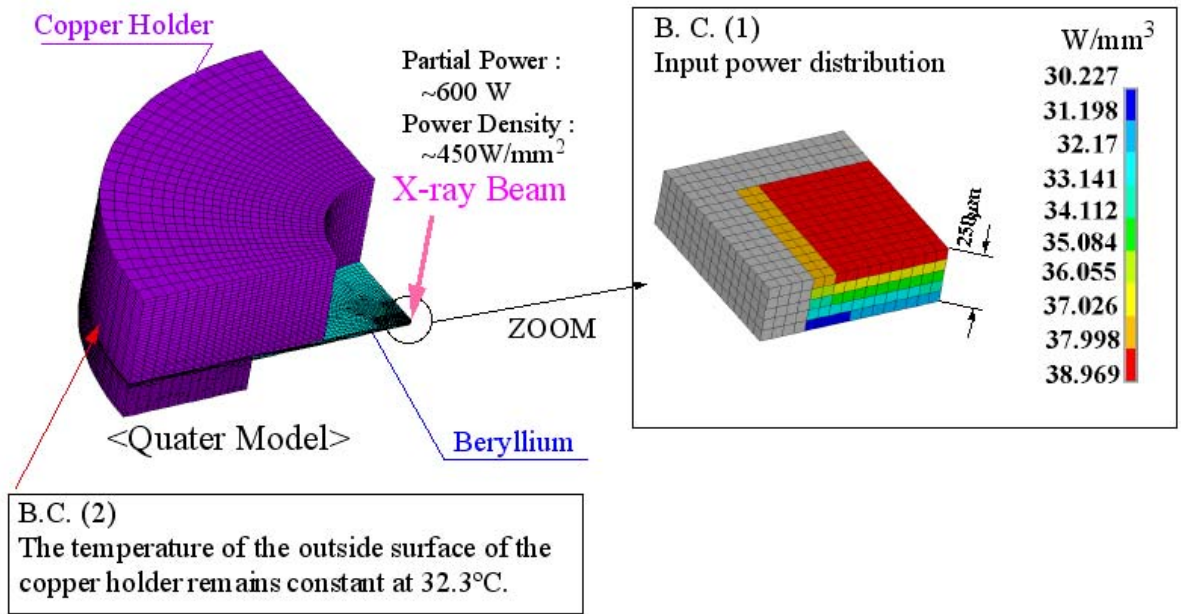


Figure 4: Quarter FEM model and the detail of the meshing for the absorbing region. Boundary conditions are also specified.

### 3.2. Steady-State Analysis

Figure 5 shows the solutions of the temperature and the resultant equivalent stress distributions calculated by the conventional steady-state analysis, which doesn't take into account a plastic deformation. The maximum temperature of the foil center is about 150°C, and the maximum equivalent stress is about 20 kgf/mm<sup>2</sup> (200 MPa). As compared with the tensile test results specified in Table 2, the maximum equivalent stress exceeds the 0.2% proof stress of TYPE B. However, the real maximum equivalent stress doesn't reach 200 MPa, because a yielding was not considered. So, we tried to carry out an elastic and plastic analysis so that the actual behavior of stresses and strains can be found and the life of the beryllium window can be estimated. So far as we know, there is hardly any example of such a trial.

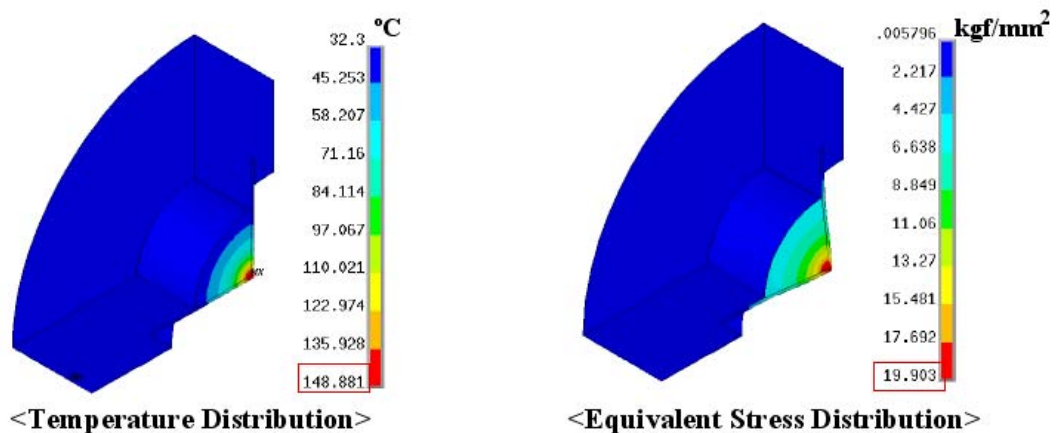


Figure 5: Temperature and resultant equivalent stress distributions for the beryllium window on the maximum heat load condition for the SPring-8 standard in-vacuum undulator. The maximum equivalent stress of about 200 MPa exceeds the 0.2% proof stress of the material.

### 3.3. Elastic and Plastic Analysis

#### 3.3.1. Preparations

Before starting a solution of the elastic and plastic analysis, we should prepare some boundary conditions. The first one is the cyclic thermal load, which is calculated by a transient thermal analysis. Figure 6 shows the transient nodal solution of the maximum temperature. To simulate a rapid heating and a rapid cooling caused by an open-close operation of the main beam shutter, the total input power was applied and removed within both 10 msec by means of ramp load. One cycle period consists of a thermal loading condition of 5 sec and an unloading condition of 5 sec. We applied fifteen cycles repeatedly.

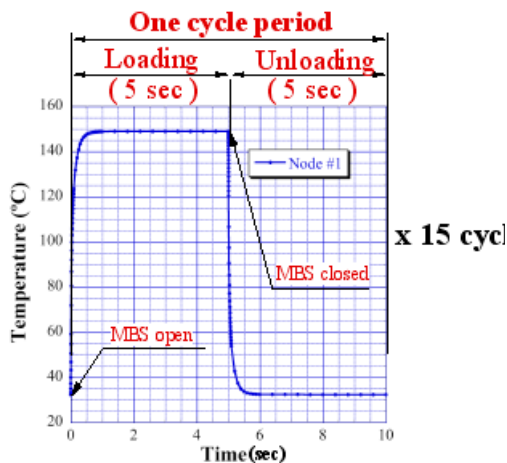


Figure 6: One cycle period of the transient nodal solution for the maximum temperature

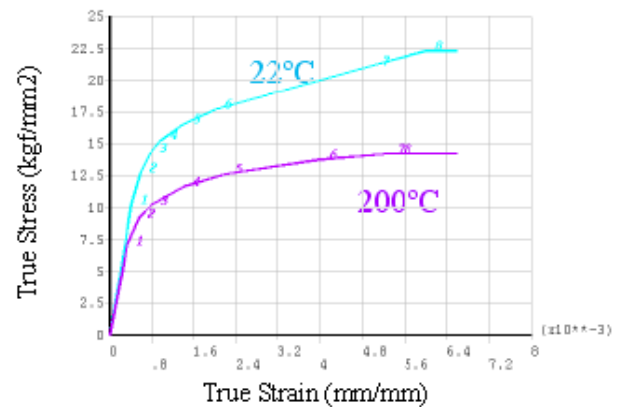


Figure 7: Stress-Strain diagram from the tensile test

The next setting parameter is the hardening rule, which will decide a change of yield surface. In general, for such a cyclic loading of compressive and tensile stresses as this case, they recommend to select the kinematic hardening rule, which the center of yield surface would move with evolution of hardening, whereas the shape of the yield surface would not change. This rule considers the Bauschinger effect. The true stress and true strain diagram of the material should also be prepared. In ANSYS solution, using the tensile test results, we defined the temperature-dependent diagrams both at 22 and 200°C, approximated by multi straight lines, as shown in Figure 7.

#### 3.3.2. Results

Figure 8 shows the solutions on the elastic and plastic analysis, which is the cyclic diagram of the equivalent stress and the equivalent plastic strain. It was plotted by element solutions where the maximum equivalent stress occurred at the steady-state analysis. It was confirmed that the diagram doesn't show a hysteresis loop even after 15 cycles, namely a plastic shakedown didn't occur, but ratcheting occurred. The tendency of the cyclic diagrams for other elements around the aimed one is almost same as

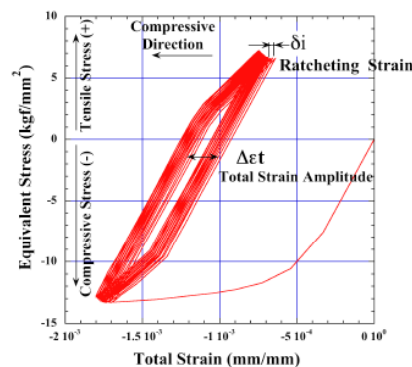


Figure 8: Cyclic diagram of the equivalent stress and the equivalent plastic strain They are marked +/- sign based on the analysis results.

the diagram of Figure 8.

Therefore, we have to estimate the life of the window from the viewpoints of both fatigue and ratcheting effect.

The width between the maximum and the minimum total strain in each cycle, which is called the total strain amplitude of  $\Delta\epsilon_t$ , is an important value for the estimation of the fatigue life. The change in  $\Delta\epsilon_t$  with cycles, plotted in Figure 9, is estimated at  $1.06 \times 10^{-4}$ . On the other hand, the

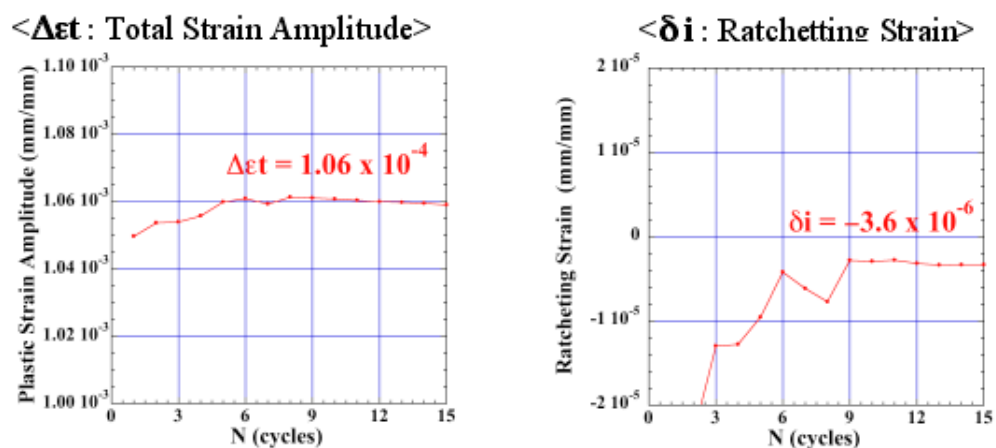
ratcheting strain of  $\delta_i$ , which is the movement of the maximum total strain in each cycle, is

Figure 8: Cyclic diagram of the equivalent stress and the equivalent plastic strain. They are marked +/- sign based on the analysis results.

estimated at just a little amount of  $-3.6 \times 10^{-6}$ . The minus sign means that the ratcheting moves toward a compressive direction.

### 3.3.3. Evaluation

We evaluated the fatigue life using the following equation, called the Manson's universal



es.

$$\Delta \epsilon_t = \left( \frac{3.5 \sigma_B}{E} \right) N_f^{-0.12} + \epsilon_f^{0.6} N_f^{-0.6}$$

slope rule, which can predict a fatigue life by a first-order approximation

using only mechanical properties of the material.

The total strain amplitude of  $\Delta\epsilon_t$  consists of the elastic strain amplitude and the plastic strain amplitude, which are described by the first and the second terms on the right-hand sides of the equation, respectively. In general, they say that this rule is fairly reliable on condition that the maximum temperature would not reach a value, at which the influence of oxidation or creep should be considered. According to the Manson's universal slope rule, we plotted two diagrams for both temperatures using the tensile test results, as shown in Figure 10. The green line shows the relationship between the total strain amplitude and the life. The fatigue life is indicated by the intersection of the green line and the line of  $\Delta\epsilon_t$  equals to ANSYS solution of  $1.06 \times 10^{-4}$ , which is estimated at one million cycles for both temperatures. Assuming that the thermal cycle is 1000 cycles per year (4 cycles per day x 250 days per year), this estimated life corresponds to a thousand year life. This life is considered to be too enough for the usage. On the other hand, as to the ratcheting effect, we have concluded that it would not affect on the life of the window because of the following reasons: 1) as the change of the ratcheting strain is just a little amount of the order of  $10^{-6}$ , we guess the ratcheting would occur due to a roughness of the meshing size. Furthermore, 2) as the ratcheting moves toward a compressive direction, it would not influence on the life essentially.

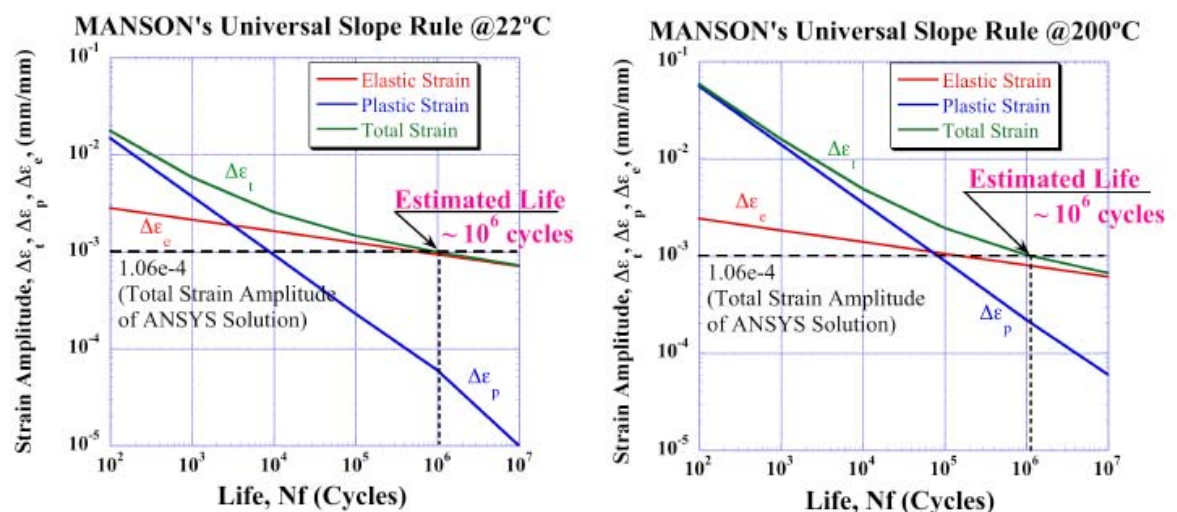


Figure 10: Relationship between the life and the strain amplitudes plotted by Manson's universal slope rule for both room temperature and 200°C.

#### 4. Conclusions and Future Plans

We have conducted an elastic and plastic analysis successfully against the new type beryllium window having the high-purity and fine-roughness but low-strength beryllium foil. The Analysis solutions indicate that the fatigue life of the window is estimated at one million cycles, according to the Manson's universal slope rule. This life is considered to be too enough for the usage. We are now trying to evaluate the life of the other high-heat-load front-end components, such as absorbers and slits, by linking the elastic and plastic analysis with experiments.

#### 5. References

- [1] M. Yabashi, K. Tamasaku, and T. Ishikawa, PHYSICAL REVIEW A **69**, 023813 (2004).